

Article

Selective Recovery of Copper from the Mixed Metals Leach Liquor of E-Waste Materials by Ion-Exchange: Batch and Column Study

Emmanuel A. Ajiboye ¹, V. Aishvarya ² and Jochen Petersen ^{1,*}

¹ Department of Chemical Engineering, University of Cape Town, Rondebosh 7700, South Africa; emmanuel.ajiboye@uct.ac.za

² Hydro & Electrometallurgy Department, CSIR-Institute of Minerals and Materials Technology, Bhubaneswar 751013, India; aishvarya@immt.res.in

* Correspondence: jochen.petersen@uct.ac.za

Abstract: Recovery of metals from e-waste forms a major focus of circular economy thinking and aligns well with the Sustainable Development Goals (SDG). While hydrometallurgical extraction from electronic printed circuit boards (PCBs) is well established, the separation of metals from the leach liquors, which are complex mixtures, remains a challenge. To achieve selective separation, ion exchange resins with chelating functional groups were employed in the present study. Batch and column studies for selective recovery of Cu^{2+} from a given mixed metals leach solution were conducted using Dowex M4195 resin, and both the adsorption isotherm and kinetics were studied. The process involves three major steps: selective recovery of Cu^{2+} by M4195 at low pH and elution with H_2SO_4 ; sorption of Ni^{2+} from the raffinate by Dowex M4195 at pH 2 and removal of Fe^{3+} from raffinate. The batch experimental results showed appreciable and selective recovery of copper (51.1%) at pH 0.7 and 40.0% Ni^{2+} was sorbed from raffinate at pH 2.0 with co-adsorption of Fe^{3+} as impurity. The batch adsorption data could be fitted with both Langmuir and Freundlich isotherms and exhibited pseudo-second-order kinetics. Column studies agreed with the Yoon–Nelson model and indicated that Cu^{2+} break-through time in the column decreased with an increase in flowrate from 3.0 to 10.0 min/mL and decreased in sorption capacity, while it was delayed with increased bed heights from 20 to 30 mm. Complete elution of Ni^{2+} was obtained with 2.0 M H_2SO_4 after selective elution of trace impurities with dilute HCl. Iron in the raffinate was removed via the addition of $\text{Ca}(\text{OH})_2$ at pH 4.0 leaving Zn-Al in the solution.

Keywords: e-waste; leaching; ion exchange; metal separation; Dowex M4195



Citation: Ajiboye, E.A.; Aishvarya, V.; Petersen, J. Selective Recovery of Copper from the Mixed Metals Leach Liquor of E-Waste Materials by Ion-Exchange: Batch and Column Study. *Minerals* **2023**, *13*, 1285. <https://doi.org/10.3390/min13101285>

Academic Editor: Rajesh Kumar Jyothi

Received: 1 September 2023

Revised: 28 September 2023

Accepted: 29 September 2023

Published: 30 September 2023



Copyright: © 2023 by the authors. Licensee MDPI, Basel, Switzerland. This article is an open access article distributed under the terms and conditions of the Creative Commons Attribution (CC BY) license (<https://creativecommons.org/licenses/by/4.0/>).

1. Introduction

Globally, waste electrical and electronic equipment (WEEE) remains the fastest growing and most complex solid waste stream. Its annual production was 52.2 M metric tons in 2019 and is further projected to reach over 74.7 M metric tons by 2030 [1,2].

WEEE contains a significant number of valuable metals which are used for electrical contacts and conduits owing to their excellent chemical stability coupled with good conducting properties [3]. Disposal of these components as waste represents both a loss of value and a potential hazard to the environment through the long-term leaching of heavy metals. Both these concerns have encouraged the recycling of e-waste to recover the metal values and safely dispose of the residues. There has been much effort towards the development of a viable approach to recycling e-waste via pyro- and hydrometallurgy routes. Acid leaching of metals from primary and secondary materials produces a liquor containing mixed metals including iron, which presents a significant problem because it has low value and at the same time interferes with the recovery of the value metals; it has been identified to be particularly problematic in electro-winning or electrochemical

deposition of metals [4–6]. Traditionally, precipitation by increasing pH to remove heavy metals is a common practice as a purification process [7–10]. However, this approach is known to generate sludges that are increasingly difficult to dispose of because of potential contamination of the environment by the heavy metals contained therein, as well as significant reagent costs associated with the necessary pH control [11]. Since there is always a loss of metal values when removing iron by precipitation [10,12], it is highly desirable to selectively recover the metal of interest prior to precipitation. Although solvent extraction (SX) is a common method used to purify and enrich copper from WEEE acidic leach liquors, iron would have been removed by precipitation before SX and would hence result in a loss of value metal [13–19]. Solvent (co-)extraction of iron mostly proceeds in the pH range of 2.5–3.5 [14,17,18], and oxalic acid, which is conventionally used in its stripping, is difficult to regenerate making the process expensive. More so, numerous setbacks such as solvent flammability, crud formation and poor phase separation are associated with solvent extraction [20]. Scale-up of solvent extraction requires well-designed mixer-settlers which are cost-intensive and need a skilled operation to mitigate the risk of solvent flammability and third-phase formation resulting in poor separation. Given these drawbacks, ion exchange resins, especially those with chelating properties, seem to have better loading capacity, are easy to operate and inexpensive. These resins possess specific functional groups that enable highly selective metal uptake. For example, resin functionalized with end groups such as bispicolylamine, amidoxime, 8-hydroxyquinoline, dithiocarbamate, diphosphonic, iminodiacetate, aminophosphonic, sulphonic, thiol, thiourea and carboxyl resins, are commercially available [21,22]. It is noteworthy that bis(2-pyridylmethyl) amine, methylglucoamine, and thiol resins are found to be most suitable for the recovery of base metal ions (such as Cu, Ni, Fe, Pb, etc.) from acidic conditions [3]. Iminodiacetic and picolylamine resin have been reported to exhibit good performance for the recovery of copper and nickel in chloride and sulfate media, with the former showing preference for nickel over copper [23–26]. However, optimization of parameters for selective recovery of metals from polymetallic liquor onto resins is not extensively available in the literature.

For our study, Dowex M4195, an amine-based chelating resin, was chosen due to reported advantages such as high selectivity towards copper in extremely acidic conditions [27,28]. The targeted metal recovery was from sulphuric acid media, as this was the preferred method for primary WEEE leaching, owing to the low solubility of solder material (Pb and Sn) [29,30], which could interfere with uptake of metal of interest [11,31]. This research focused on the selective recovery of Cu^{2+} ions and removal of impurities from mixed metal sulfuric acid leach liquor of waste electronic materials using Dowex M4195 resins via fixed bed column and builds on a previous study [32].

2. Materials and Methods

2.1. Sorbate and Chelating Resin Characteristics

Numerous articles have been published on the sorption of Cu^{2+} from simplified and often pure solutions, whereas in practice the leach liquor would always contain multiple metals that can co-extract. Therefore, for this study, the leach liquor obtained from our previous leaching of metals from waste electrical components was used [33], with the typical chemical composition presented in Table 1. The initial pH of the liquor was 0.33 (2.0 M H_2SO_4).

Table 1. Composition of sulfate leach liquor of waste electrical materials.

Metals	Cu	Ni	Mn	Fe	Zn	Al	Sn	Pb
Concentration (mg/L)	5230	312	90.9	1220	477	305	5.50	2.01

Given the limited availability of resin for this study, the leach liquor was diluted to the desired initial concentrations prior to the sorption experiments, and pH adjustment was executed using dilute H_2SO_4 and NaOH solutions. The reagents used (H_2SO_4 , NaOH,

H₂O₂, and Ca (OH)₂) were all analytical-grade reagents. The selection of resin was based on the metal compositions of the leach solution, as well as its availability, cost, and physico-chemical properties. Dowex M4195 is a chelating resin with a multidentate amine ligand and microporous structure. It is a polystyrene-divinylbenzene opaque bead appearing tan to dark brown or dark green [34]. According to the product information given by the manufacturer, the resin functionality is based on a special chelating amine ligand which is partially quaternized by sulfuric acid. In this conjugate sulfuric acid salt form, the resin is fully swollen and hydrated, and ready for scavenging metals from acidic media even in the presence of other chelating agents such as EDTA. It is recommended for the removal of transition metals at pH < 2.0. Detailed molecular-level characterization of Dowex M4195 in the context of Cu removal has been given in a recent publication [28].

2.2. Experimental Procedure

The experimental program included the following major steps:

- Batch experiments for copper adsorption and elution using Dowex M4195 with determination of isotherms.
- Fixed bed adsorption and desorption studies of Cu²⁺ ions.
- Treatment of raffinate for the removal of Ni²⁺ using spent Dowex M4195 and removal of Fe³⁺ from solution.

2.2.1. Batch Experiment

Both sorption and desorption of metals onto or from Dowex M4195 resin was conducted using an orbital shaker at 200 rpm. In an Erlenmeyer flask, 200 mg of preconditioned (washed with 1.0 M H₂SO₄) Dowex M4195 resin was contacted with 50 mL of sulfate leach solution. The pH of mixed metals sulfate leach solution, equilibration time and mass ratio of resin to leach solution are the parameters used to evaluate the batch recovery efficiency. After sorption, the metal content in the solution was determined by Atomic Absorption Spectrometry (AAS) using a Perkin Elmer Analyst 200 (Perkin Elmer, Rodgau, Germany). The recovery efficiency of metal from leach solution (%R) was calculated by Equation (1), and the percentage of metal stripped (%S) was determined by Equation (2).

$$\%R = \frac{(K_0 - K_t)}{K_0} \times 100 \quad (1)$$

where K_0 and K_t represent the concentration of metals at times 0 and t , respectively (mg/L).

$$\%S = \frac{Q_s}{Q_a} \times 100 \quad (2)$$

where Q_s is the amount of metal stripped from the loaded resin, and Q_a is the amount of metal adsorbed onto resin before stripping (mg/g).

2.2.2. Fixed Bed Sorption Study

After the determination of optimum pH for adsorption, selective sorption of Cu²⁺ was investigated via fixed bed column experiments. The column was made from a Perspex tube with dimensions of 15 mm diameter and 205 mm length. The sampling point was located at the bottom tip of the column. The column was packed with preconditioned Dowex M4195 resin using glass wool as a supporting layer above and below the resin bed. The mixed metals pregnant leach solution at optimized pH was pumped through the column with a peristaltic pump from top to bottom. The effluent was collected at regular time intervals using a calibrated plastic sampler, and the metal ion concentration in the solution was determined by AAS. The column performance towards selective sorption of copper onto Dowex M4195 resin was investigated as a function of flow rate (3.0, 5.0, and 10.0 mL/min) and bed depth (20, 25, and 30 mm). After sorption, the column was eluted with 2.0 M H₂SO₄ solution.

Fixed bed column parameters for the sorption of copper by Dowex M4195 resin were evaluated in terms of breakthrough time and total sorption (q_t) of the resin. The loading behavior of metals onto resin in the column was expressed in terms of concentration C_t/C_0 as a function of time (t), where C_0 and C_t are the concentrations of inlet mixed metals solution and outlet concentration at time t , respectively and breakthrough curves were plotted, column exhaustion time and total effluent volume (V_e , mL) was calculated from the following equation:

$$V_e = Q \times t_{total} \quad (3)$$

where Q (mL/min) and t_{total} (min) are the volumetric flow rate and the time of exhaustion, respectively. With a known solution concentration and flow rate, the area of the breakthrough curve was determined via integration of the adsorbed concentration ($C_0 - C_t$) versus t (min) curve. The sorption parameters (Equations (4)–(6)) were estimated according to [35]. The total sorption q_t (mg) was obtained from Equation (4):

$$q_t = \frac{QA}{1000} = \frac{Q}{1000} \int_{t=0}^{t=t} (C_0 - C_t) dt \quad (4)$$

The equilibrium maximum copper sorption capacity (q_e , mg/g) of the column was calculated using Equation (5), where m (g) is the weight of resin beads in the column.

$$q_e = \frac{q_t}{m} \quad (5)$$

The total amount of metal ions (m_t) entering column (mg) was calculated according to Equation (6):

$$m_t = \frac{C_0 \cdot q_t}{1000} \quad (6)$$

The Cu^{2+} sorption efficiency (R %) at resin saturation was calculated based on Equation (7):

$$R(\%) = \frac{q_t}{m_t} \quad (7)$$

2.2.3. Column Sorption Models

Thomas Model

The Thomas model is applied to experimental data for the evaluation of breakthrough fitting, regardless of sorption equilibrium, and it is based on a Langmuir isotherm. The linearized form of the model is expressed as per Equation (8).

$$\ln\left(\frac{C_0}{C_t} - 1\right) = \frac{k_{Th}q_0m}{Q} - k_{Th}C_0t \quad (8)$$

where k_{Th} is the Thomas kinetic coefficient (mL/min/mg), t is the total flow time (min), and Q is the volumetric flow rate (mL/min). The adsorption capacity and mass of the adsorbent are denoted as q_0 (mg/g) and m (g). A plot of $\ln[(C_0/C_t) - 1]$ versus t gives the value of k_{Th} and q_0 .

Yoon–Nelson Model

The Yoon–Nelson model assumes that the rate of sorption of Cu^{2+} ions is inversely proportional to the extent of Cu^{2+} already sorbed and breakthrough on the resin. It is expressed as Equation (9).

$$\ln\left(\frac{C_t}{C_0 - C_t}\right) = k_{YN}t - \tau k_{YN} \quad (9)$$

where τ is the time required for 50% adsorbate breakthrough (min), t is sampling time (min), and k_{YN} is the rate constant (1/min).

2.2.4. Sorption of Nickel and Removal of Impurities

The raffinate obtained after copper elution was completely recovered and adjusted to pH 2.0 and the spent resin was packed and the raffinate solution was pumped through the column. Iron left in the solution was removed by precipitation with $\text{Ca}(\text{OH})_2$ prior to the discharge of the solution.

3. Results and Discussion

3.1. Batch Sorption Study

The pH plays a significant role in the affinity of a resin for a particular ion. Hence, the effect of pH on the recovery of metals from the multi-metallic pregnant leach solution was studied to determine optimal conditions. As shown in Figure 1, Dowex M4195 resin performed excellently for the recovery of Cu^{2+} in the highly acidic range. Recovery of Cu^{2+} becomes less selective at $\text{pH} > 0.7$, at which point the recovery efficiency of other metals becomes more prominent. This is plausible because only one nitrogen atom of the bis-(2-pyridylmethyl) amine functional group is deprotonated and has a strong affinity for Cu^{2+} at highly acidic conditions. On the other hand, in the mid to high pH range, two or all the nitrogen atoms of bis-(2-pyridylmethyl) amine functional groups are deprotonated and thus show increased affinity to other metals [34].

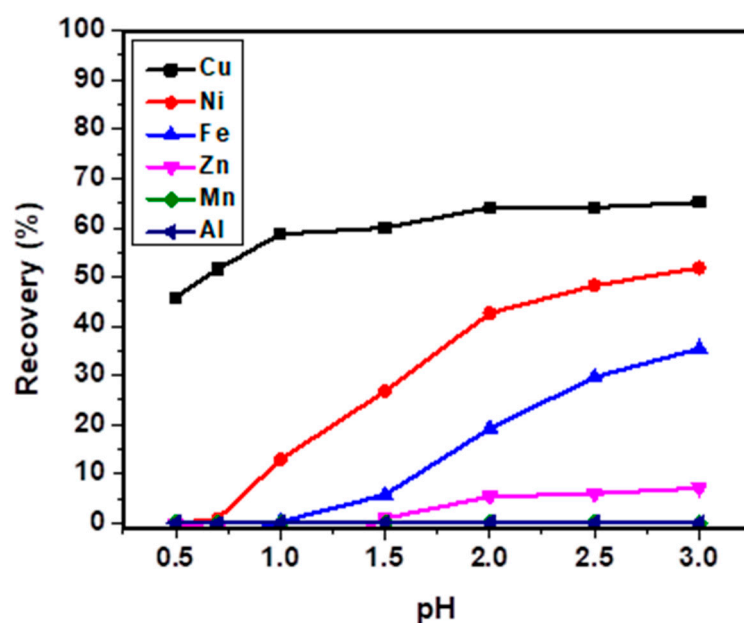


Figure 1. pH studies [Resin/solution ratio: 4 g/L, Cu—209.13 mg/L, Ni—11.1 mg/L, Fe—54.7 mg/L, Zn—20.6 mg/L, Mn—4.2 mg/L and Al—7.5 mg/L, time—180 min, stirring—200 rpm, and 25 °C].

Therefore, pH 0.7 was found to be optimum for the selective sorption of copper. Our results were in consonance with other sources [11,36], who reported that Dowex M4195 still retains its affinity for metals in highly acidic medium. Subsequently, equilibrium recovery time was studied at the optimal pH and the result shows that the selective recovery efficiency of Cu^{2+} steadily increased when the time increased from 5 to 120 min and reached equilibrium after 180 min without sorption of other metals (Figure 2). A 51.1% recovery efficiency was achieved at optimal time at the given resin loading (4.0 g/L). When the mass of resin in the solution was increased to 10.0 g/L, the recovery efficiency of Cu^{2+} increased and reached 90.5% at 180 min (Figure 3).

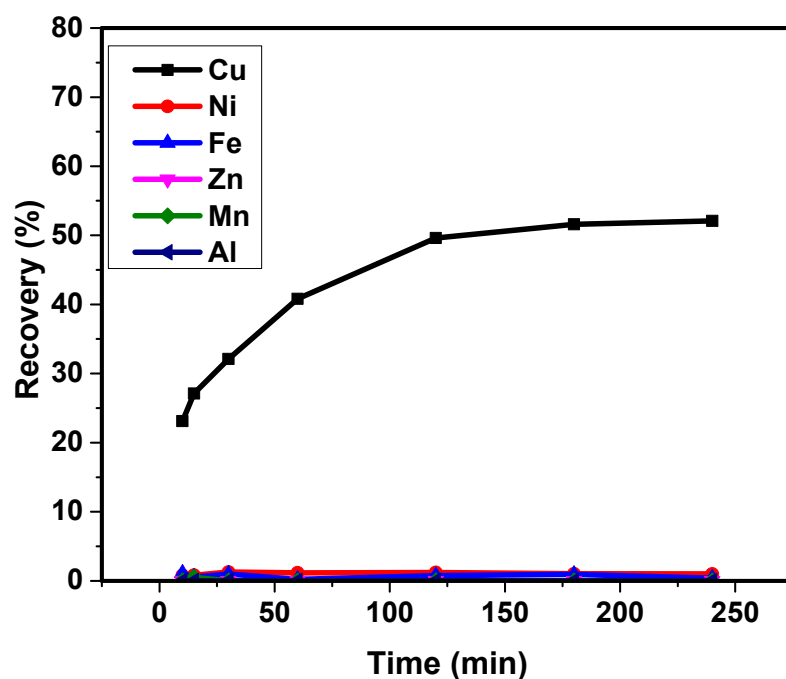


Figure 2. Equilibration time studies [Resin/solution ratio: 4 g/L, Cu—209.13 mg/L, Ni—11.1 mg/L, Fe—54.7 mg/L, Zn—20.6 mg/L, Mn—4.2 mg/L and Al—7.5 mg/L stirring—200 rpm, initial pH—0.7, and temperature—25 °C].

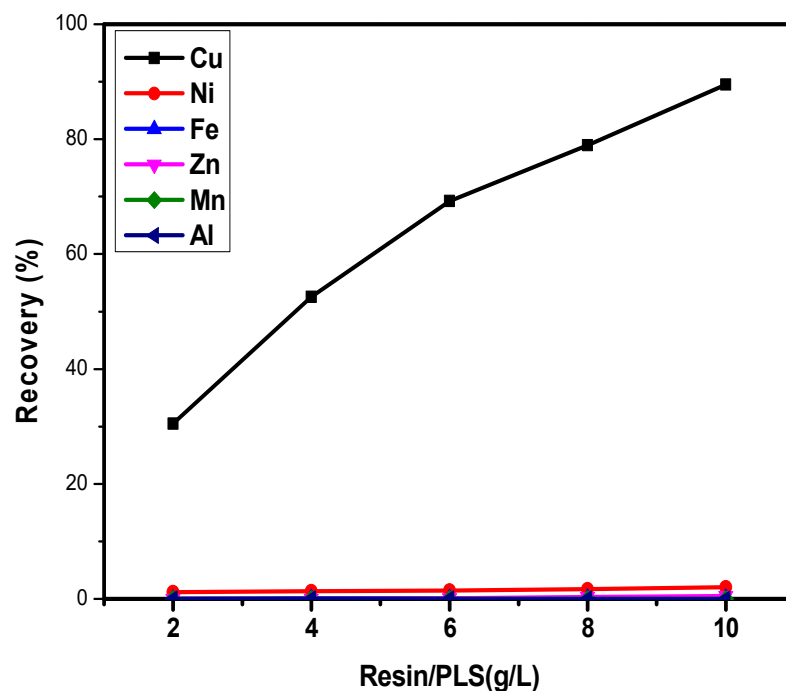


Figure 3. Plot of resin to pregnant leach solution ratio [Cu—209.13 mg/L, Ni—11.1 mg/L, Fe—54.7 mg/L, Zn—20.6 mg/L, Mn—4.2 mg/L and Al—7.5 mg/L stirring—200 rpm, initial pH—0.7, and temperature—25 °C].

3.2. Batch Sorption Isotherm

The sorption isotherm is important in the ion exchange process because it can reveal the interactive behavior between the adsorbents and ions in the solution. Therefore, the isotherm for the selective sorption of Cu^{2+} using Dowex M4195 chelating resin at the given

background concentrations of Ni, Fe, Zn and Al was studied. The batch sorption data obtained were fitted with Langmuir and Freundlich isotherm models.

3.2.1. Langmuir Isotherm

Langmuir isotherm assumes that adsorption is proportional to the fraction of the surface of the adsorbent that is open while desorption is proportional to the fraction of the adsorbent surface that is covered [37]. Equation (10) is expressed in linear form [38].

$$\frac{C_e}{Q_e} = \frac{1}{Q_m K_L} + \frac{C_e}{Q_m} \tag{10}$$

where Q_e (mg/g) is the adsorption capacity, C_e (mg/L) is the equilibrium concentration of Cu^{2+} ions, Q_m (mg/g) is the maximum Cu^{2+} ions sorption capacity, K_L (L/mg) is the Langmuir constant obtained from the plot of C_e/Q_e vs. C_e . The important parameter of the Langmuir isotherm was expressed as a dimensionless value R_L , Equation (11), called the separation factor [39].

$$R_L = \frac{1}{1 + K_L C_0} \tag{11}$$

where K_L is Langmuir constant (mg/g) and C_0 is the initial concentration of adsorbate (mg/g). When the R_L value is in the range $0 < R_L < 1$, it is an indication that the sorption of Cu^{2+} ions was favorable, unfavorable when $R_L > 1$, linear when $R_L = 1$, and irreversible when $R_L = 0$.

The sorption isotherm plot is presented in Figure 4 and the parameters calculated from fitting the plot are presented in Table 2. It is shown that the maximum sorption capacity (Q_m) is 5.89 mg/g and the separation factor R_L is < 1 , which indicates a favorable sorption process. The correlation regression coefficient is 0.99 which indicates a good fit to the isotherm.

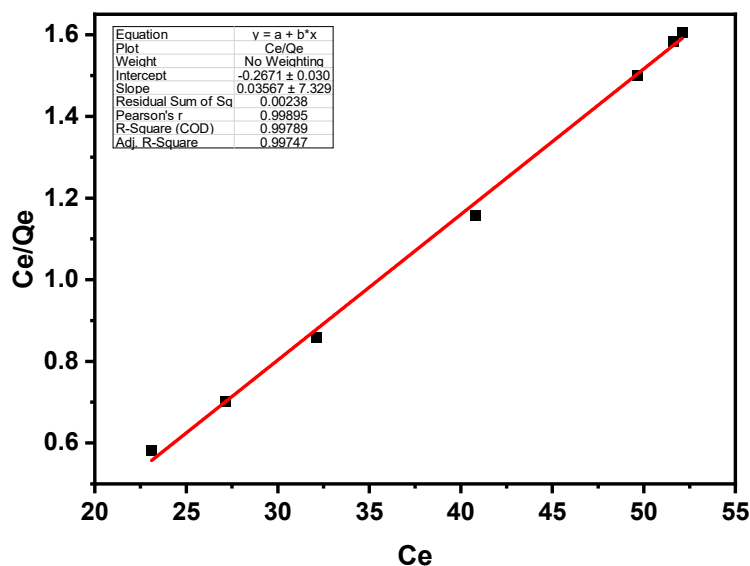


Figure 4. Langmuir plot for the sorption of Cu^{2+} ion from multi-metal leach solution by Dowex M4195.

Table 2. Estimated Isotherm Parameters.

Isotherm	Langmuir Model				Freundlich Model		
	Q_m (mg/g)	K_L (L/mg)	R_L	R^2	K_f	$1/n$	R^2
Parameters Values	5.89	3.74	0.015	0.99	36156.8	0.975	0.99

3.2.2. Freundlich Isotherm

This isotherm describes the surface heterogeneity and the exponential distribution of active sites and their energies [39]. The linear form of this isotherm is presented in Equation (12) [40].

$$\ln Q_e = \ln K_f + \frac{1}{n} \ln C_e \quad (12)$$

where K_f is the sorption capacity (L/mg), and $1/n$ is the sorption intensity; and useful to predict heterogeneity of the adsorbate sites which are obtained from a plot of $\ln Q_e$ vs. $\ln C_e$ (Figure 5). The value of $1/n$ obtained shows that at high concentrations, the relative adsorption decreases, which is indicative of the saturation of adsorption sites available.

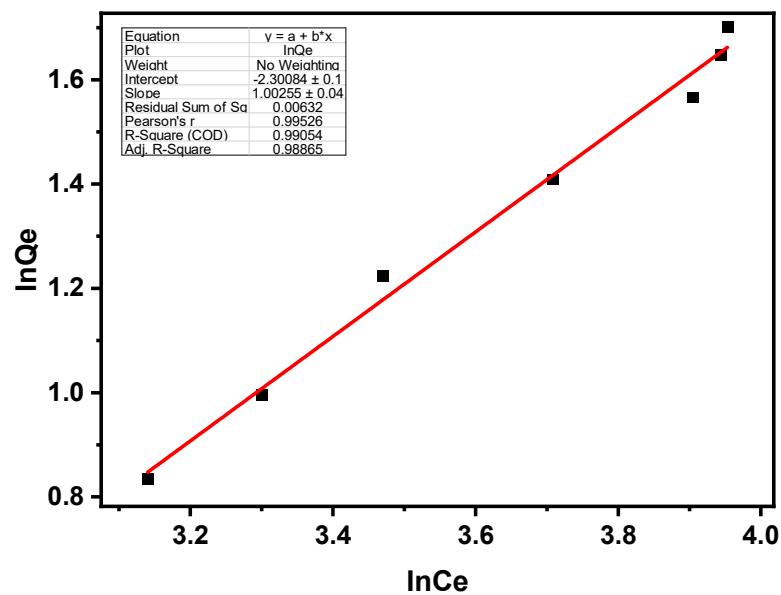


Figure 5. Freundlich plot for the sorption of Cu^{2+} ion from multi-metal leach solution by Dowex M4195.

However, the smaller value of $1/n$ and larger K_f values determined (as shown in Table 2) indicate that the sorbent has a higher sorption capacity and a strong affinity towards Cu^{2+} ions. The slight deviation from the linear at the high concentration end in the Freundlich plot indicates saturation and thus multi-layer sorption for Cu^{2+} is the less likely mechanism, despite the high correlation coefficient (R^2) for either isotherm model in the range studied.

3.3. Sorption Kinetics

The kinetics for the selective sorption of Cu^{2+} from the multi-element leach solution by Dowex M4195 were evaluated. The modeling of experimental data was performed using pseudo-first and second-order kinetics. The calculated results obtained from pseudo-first and second-order Equations (13) and (14), adapted from [41], are given in Table 3.

$$\log(Q_e - Q_t) = \log Q_e - \left(\frac{k_1}{2.303} \right) t \quad (13)$$

$$\frac{t}{Q_t} = \left(\frac{1}{k_2 Q_e^2} \right) + \left(\frac{t}{Q_e} \right) \quad (14)$$

where Q_e (mg/g) and Q_t (mg/g) are the sorption capacity at equilibrium and at time t (min), respectively; k_1 (1/min) and k_2 (g/mg/min) are the sorption rate constants of pseudo-first and second-order models. The coefficients (R^2) obtained from the plotted data for the two-kinetics models showed that the data fitted pseudo-second-order kinetics well, but a

poor fit was achieved for the pseudo-first-order plot (Figures 6 and 7). This is an indication that chemisorption occurred.

Table 3. Estimated kinetics parameters for the selective sorption of Cu²⁺ by Dowex M4195.

Kinetics	Pseudo-First Order			Pseudo-Second Order		
Parameters	Q_e	k_1	R^2	Q_e	k_2	R^2
Values	50.0	0.006	0.86	1.3	0.072	0.998

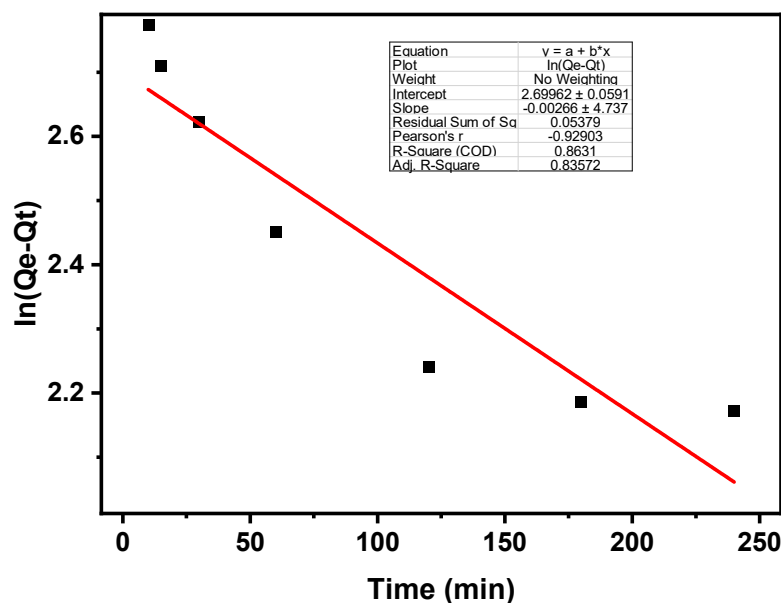


Figure 6. Pseudo first order plot for the sorption of Cu²⁺ ion from multi-metal leach solution by Dowex M4195.

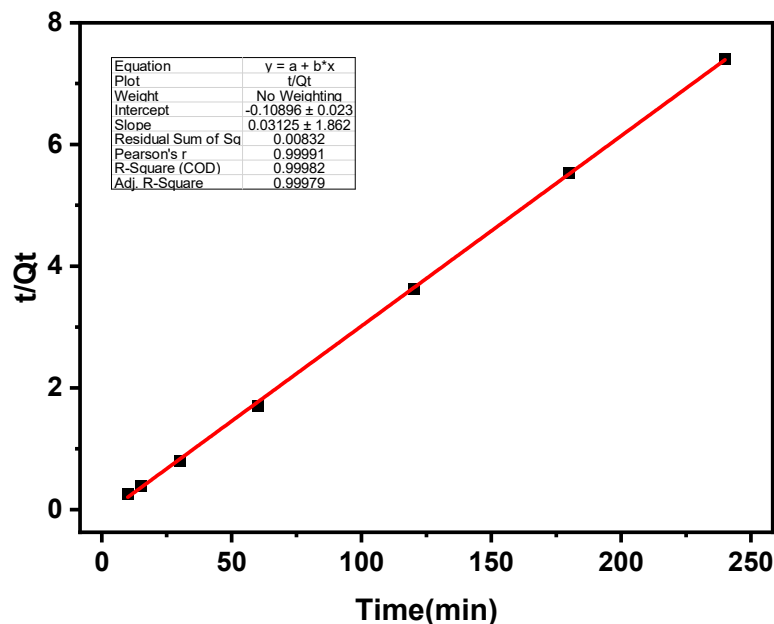


Figure 7. Pseudo second order plot for the sorption of Cu²⁺ ion from multi-metal leach solution by Dowex M4195.

3.4. Column Sorption of Copper

Based on optimal conditions obtained from the batch sorption study, a fresh stock of mixed metal leach solution was carefully diluted to give the target pH of 0.7. The

solution was then pumped into the column at a flow rate in the range of 3–10 mL/min and for varying bed height (20–30 mm), and the performance of Dowex M4195 resin for selective sorption of Cu^{2+} through the column was then evaluated. The loading behavior of metals onto the resin was expressed in terms of the concentration C_t/C_0 as a function of time (t), where C_0 and C_t are the concentrations of metals in the inlet and outlet at time t , respectively.

3.4.1. Effect of Flow Rate on Breakthrough Curve

The plots of breakthrough curves are presented in Figure 8. It is evident that the breakthrough of Cu^{2+} (i.e., its detection in the effluent) occurs almost instantaneously due to the short length of the resin bed (20 mm). The time for Cu^{2+} adsorption to cease completely (resin saturation) decreased with increases in flow rate from 3 to 10 mL/min, as expected. Thus, Cu^{2+} ion sorption attained saturation at 180 min with a flow rate of 3 mL/min, whereas when increased to 5 and 10 mL/min, saturation was noticed at 120 and 60 min, respectively. Further, the effect of flow rate on the breakthrough of other metal impurities was studied. The results presented in Figure 9 reveal that small amounts of Ni^{2+} were adsorbed initially but were observed to have become saturated in less than 10 min, and this time becomes even shorter as the flow rate increases (Figure 9a–c). This behavior was due to some limited interaction of Ni^{2+} ions with binding sites available on Dowex M4195 at highly acidic conditions. It is also observed that other impurities breakthrough immediately, showing minimal to no retention.

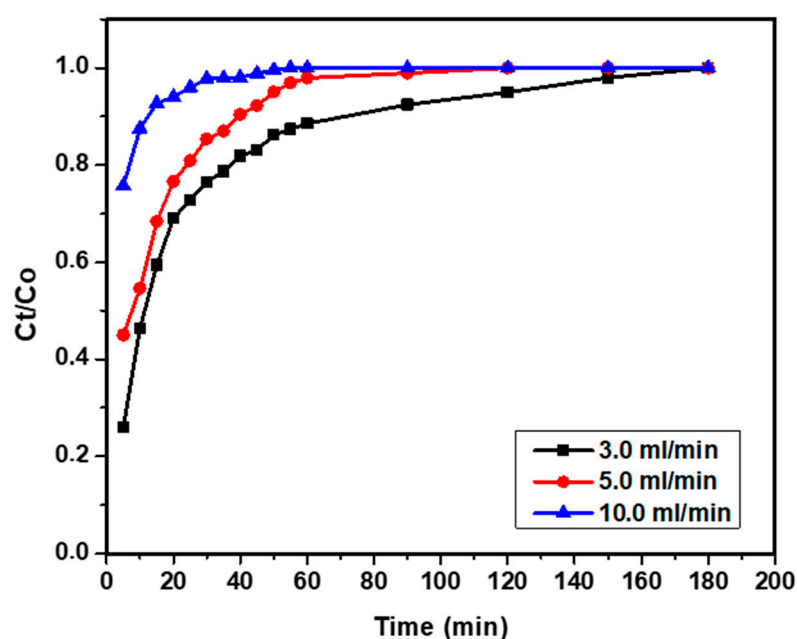


Figure 8. Effect of flow rate on the breakthrough curve of Cu^{2+} in the column; conditions are: initial concentration (Cu—1020 mg/L, Fe—305 mg/L, Ni—40 mg/L, Zn—41.5 mg/L, and Mn—12.05 mg/L), temperature—25 °C and pH = 0.7.

3.4.2. Effect of Bed Height on Breakthrough Curve

Conversely, an increase in the mass of resin (bed height) slightly delayed both the breakthrough point of Cu^{2+} through the column and the time to reach saturation (Figure 10). When the bed height was increased from 20 to 25 mm, Cu^{2+} saturation points were noticed at 90 and 120 min. Further increasing the bed height from 2.5 to 3.0 cm led to further lengthening of breakthrough time to 180 min. A limited number of different bed heights were used due to the limited quantity of resin available for the test work.

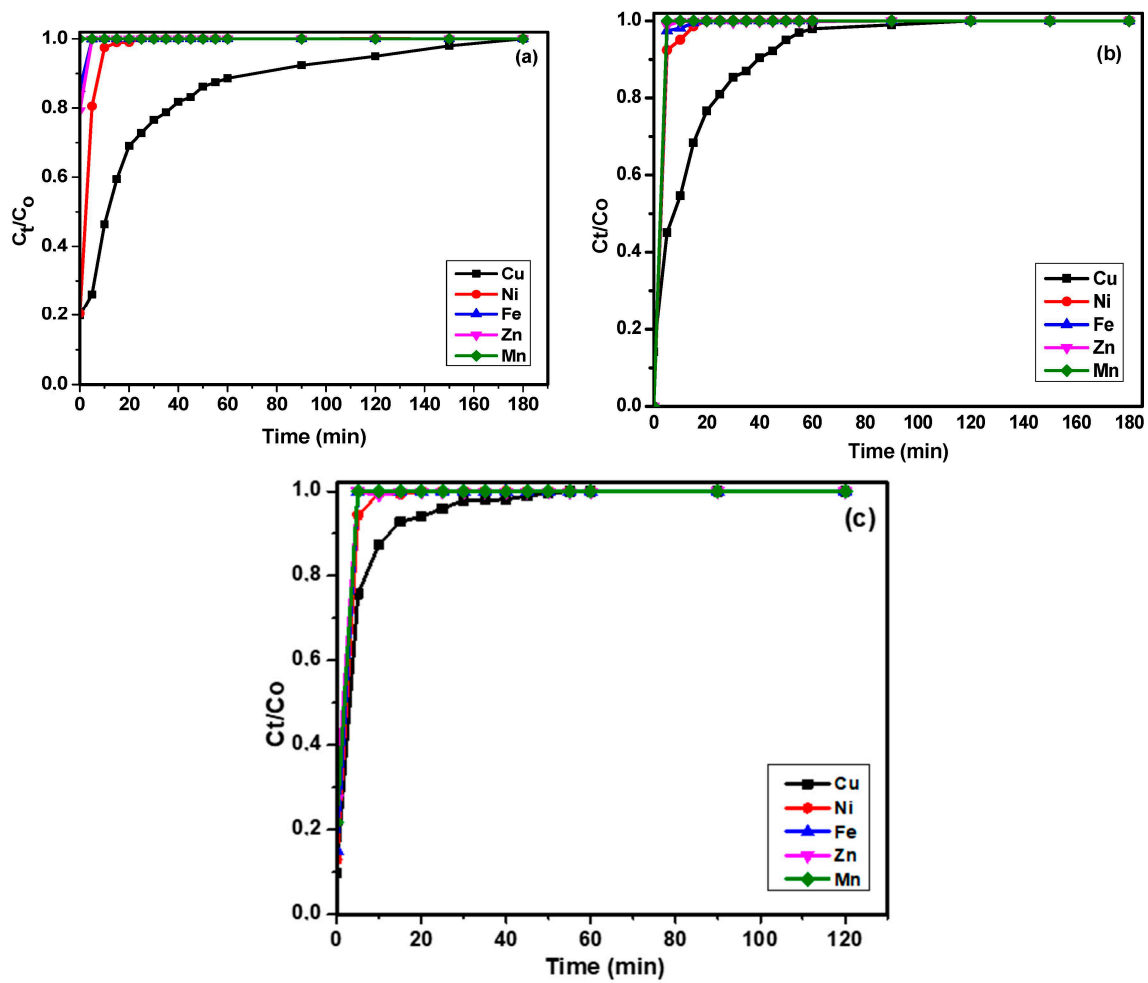


Figure 9. Effect of flow rate on the breakthrough curve of other metals as compared to Cu^{2+} in the column: (a) 3 mL/min flowrate, (b) 5 mL/min flowrate and (c) 10 mL/min; conditions are: initial concentration (Cu—1020 mg/L, Fe—305 mg/L, Ni—40 mg/L, Zn—41.5 mg/L, and Mn—12.05 mg/L), temperature—25 °C and pH = 0.7.

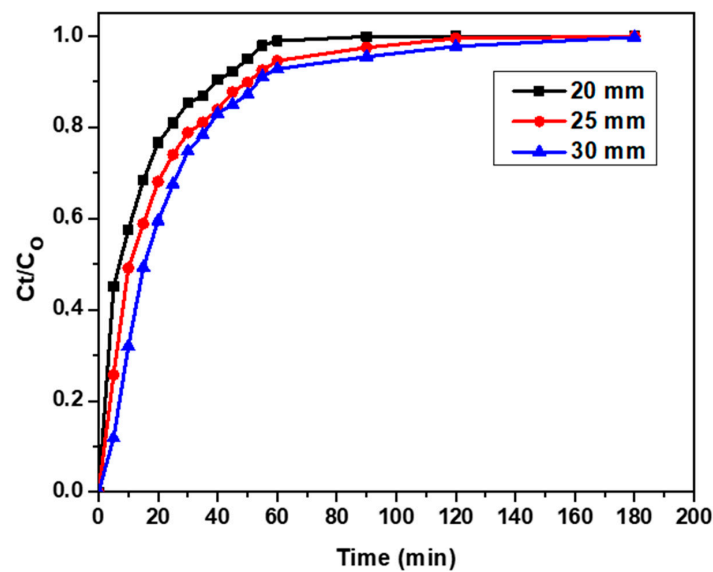


Figure 10. Effect of bed height on the breakthrough curve of Cu^{2+} in the column: conditions are: initial concentration (Cu—1020 mg/L, Fe—305 mg/L, Ni—40 mg/L, Zn—41.5 mg/L, and Mn—12.05 mg/L), flow rate—5 mL/min, temperature—25 °C and pH = 0.7.

3.5. Determination of Column Parameters

Sorption experimental data obtained based on the flow rate and bed height were substituted into Equations (3)–(7), and the evaluated results are presented in Table 4. It is shown that the sorption capacity (q_e) decreases with increases in flow rate and slightly increases when bed height (mass of resin) is increased. The decrease in the amount of Cu^{2+} ions uptake by the resin (q_t) as the flow rate increases from 3 to 10 mL/min is a result of a low retention or contact time for Cu^{2+} ions to interact with charged resin, coupled with slower diffusion of Cu^{2+} ions into the resin binding sites. Similar results have been observed in the literature albeit under different experimental conditions in terms of sorbents, solutions, and concentrations [42–47]. However, this behavior was observed to affect the sorption efficiency of Cu^{2+} which decreases with higher flow rates, because desorption of already adsorbed Cu^{2+} ions onto resin is possible at higher flow rates. The result, however, revealed that the best way to increase the residence time is to decrease the flow rate and increase the bed height. This is proven as total sorption (q_t) and the sorption efficiency (%R) for Cu^{2+} increased as bed height increased from 2.0 to 3.0 cm and decreased with flow rate from 10 to 5 mL/min.

Table 4. Calculated column parameters for the recovery of copper by Dowex M4195.

<i>H</i>	C_0	<i>Q</i>	q_t	m_t	q_{eq}	C_{eq}	%R
20	1099	3	19.8	494.6	19.8	1055.5	4
20	974	5	17.4	541.4	17.4	945	3.2
20	924.5	10	3.6	554.7	3.6	918.5	0.7
25	894.5	5	20.1	536.7	10.1	861	3.8
30	902	5	27.4	541.5	11.0	865.5	4.1

C_0 —influent concentration (mg/L), Q —flow rate (mL/min), H —bed height (mm), q_t —adsorption at breakthrough (mg g^{-1}), q_{eq} —adsorption at saturation (mg/g), m_t —total amount of Cu^{2+} ions, %R—total Cu^{2+} sorption at saturation (%).

3.6. Batch and Column Desorption

In the literature, the NH_3 solution was reported to be effective for the desorption of Cu^{2+} from Dowex M4195 [31]. However, the complexation of NH_3 and Cu^{2+} in the form of cupric amine ($[\text{Cu}(\text{NH}_3)_4]^{2+}$) is unsuitable for subsequent processing in direct electrowinning to achieve a quality cathode product. Better current density and cathode product purity can be achieved from sulfate media, and this therefore makes sulfuric acid a much superior choice for copper desorption [11,48,49]. For this work, concentrated H_2SO_4 was used for the desorption of Cu^{2+} ions from Dowex M4195 resin and regenerated. Initially, batch elution studies were performed, and the results are presented in Figure 11. They show that 90% desorption of Cu^{2+} ions was achieved in 60 min using 2.0 M H_2SO_4 . Almost complete desorption of Cu^{2+} was also achieved when the strength of the desorbing solution increased further. Based on the batch elution profile, column desorption studies were conducted using 2.0 M H_2SO_4 and the result is presented in Figure 12. Instant breakthrough of the trapped impurities was observed, while the desorption rate for Cu^{2+} increased when increasing the flow rate from 5 to 10 mL/min (Figure 12a,b). This implies that the concentration of eluted copper was 1.0 g/L over the first 5 min at 5.0 mL/min and decreased to 0.27 g/L when the flow rate was changed to 10 mL/min. Cu^{2+} was completely desorbed when eluting with 2.0 molar H_2SO_4 at 10 mL/min after 120 min. The resin could be regenerated with distilled water and reused.

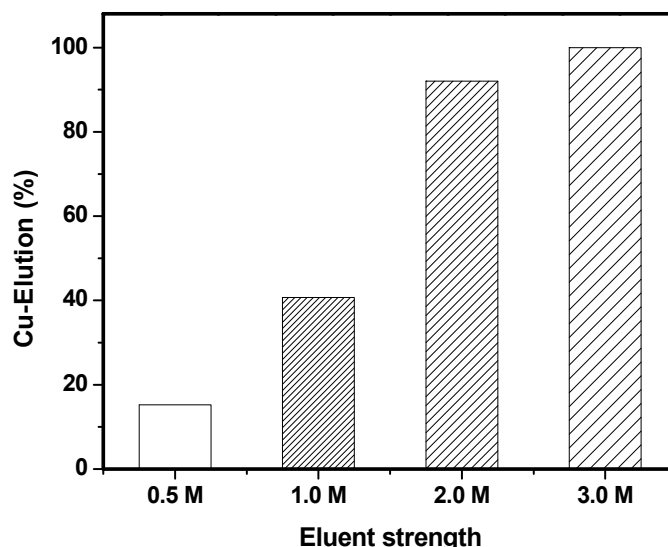


Figure 11. Batch desorption profile of Cu²⁺ ions from Dowex M4195 using different concentrations of H₂SO₄ at 25 °C for 60 min using 4.0 g/L resin/solution ratio.

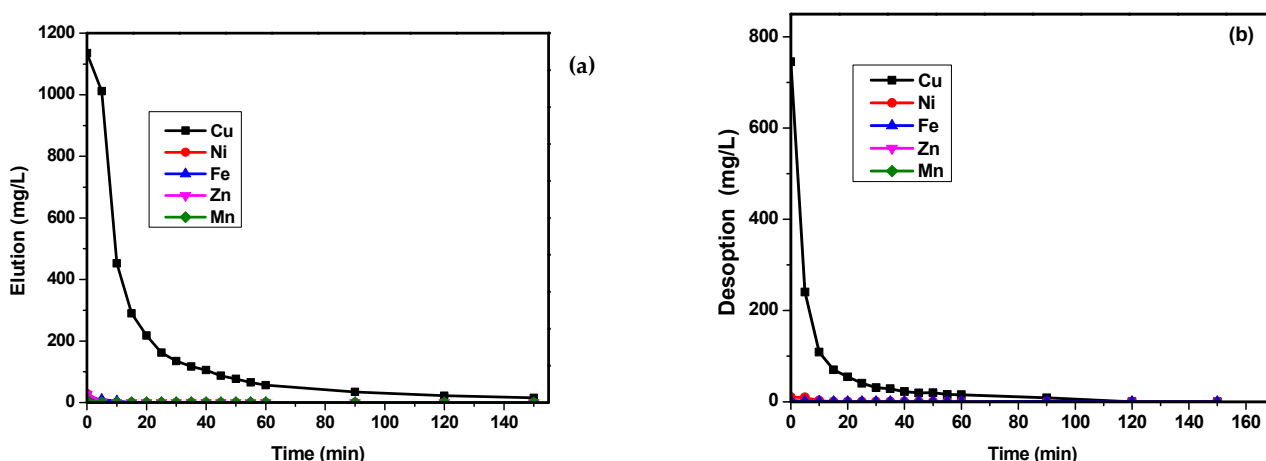


Figure 12. Column desorption of Cu²⁺ from Dowex M4195 using 2.0 M H₂SO₄ at flow rate (a) 5.0 mL/min and (b) 10.0 mL/min and resin bed—2.0 cm at 25 °C.

3.7. Modelling of Column Data

The sorption data were fitted to both the Thomas and the Yoon–Nelson model, thereafter the relevant parameters were evaluated from a plot of $\ln [C_0/C_t - 1]$ against t as shown in Equations (8) and (9). For the Thomas model, the value of sorption capacity (q_0) and rate constant (K_{Th}) were obtained from the intercept and slope. Results presented in Table 5 show that q_0 values increased with the flow rate, and slightly increased with the bed depth. Similar trends were found in the results of other scholars [50,51]. The correlation coefficient (R^2) value is approximately 0.90 which indicates the experimental data fitted the Thomas model reasonably well.

Values of the rate constant (k_{YN}), and time required for half Cu²⁺ ions concentration to break through the column (τ) were estimated from the slope and intercept of the Yoon–Nelson plots at different flow rates and bed heights as shown in Table 5. The values of k_{YN} increased with increasing flow rate and bed height. Values of τ decreased as the flow rate increased but slightly increased as bed height increased. The decrease in τ as the flow rate increases indicated that the resin bed exhausted more quickly as the flow rate increases, this behavior is evident in most sorption processes [50,52]. The value of τ (min) in Table 5 represents the time for the Cu concentration in the column effluent to reach 50% of its final level. However, a higher value of τ (min) signifies better performance of the column as

similarly reported in the literature [53,54]. Therefore, these experimental data were found to be well-fitted with the Yoon–Nelson model with R^2 values greater than 0.94. This is an indication that internal mass transfer may be the limiting step.

Table 5. Column parameters predicted by Thomas and Yoon–Nelson model for Cu^{2+} by Dowex M4195.

Column Parameters			Thomas Model			Yoon–Nelson Model		
H	C_0	Q	$k_{TH} \times 10^{-5}$	Q_0	R^2	k_{YN}	τ	R^2
2	1099	3	4.187	32.47	0.93	0.0519	11.34	0.95
2	974	5	4.663	34.1	0.91	0.0523	10	0.95
2	924.5	10	10.22	64.77	0.90	0.097	6.62	0.94
2.5	894.5	5	4.8452	39.7	0.91	0.04681	8	0.95
3	902	5	6.0798	49.01	0.92	0.05648	16.3	0.94

H = bed height (cm), C_0 is initial concentration of Cu (mg/L), Q is the flow rate (mL/min), K_{TH} is the Thomas constant (mL/mg/min), q_0 is the adsorption capacity (mg/g), k_{YN} is the Yoon–Nelson rate constant (1/min), τ is the half-breakthrough time (min) and R is the regression coefficient.

3.8. Treatment of Raffinate

After complete sorption of Cu^{2+} ions from the mixed metal sulfate liquor through multiple contacts with the resin, the pH of the raffinate was adjusted (pH 2.0) and nickel was sorbed using Dowex M4195 resin. The test work followed a similar methodology to Cu adsorption. The result obtained from batch experiments shows an increase in sorption of Ni^{2+} from 40.1 to 48.1% as the solution pH changed from 2.0 to 3.0. More so, the result presented in Figure 13 shows that Dowex M4195 sorbed Ni^{2+} with traces of Fe^{3+} which reached saturation at 120 and 20 min, respectively. A similar trend was reported in the literature, where Dowex M4195 showed strong affinity towards Ni^{2+} , and Fe^{3+} broke through the column due to its low affinity and concentration at pH 2.0 [31]. Hydrochloric acid was effective for the removal of iron sorbed onto Dowex M4195. As presented in Figure 14, different concentrations of HCl solution were tested, and 99.9% of the sorbed trace Fe^{3+} ion was selectively removed from the column by 0.2 M HCl, leaving behind the Ni^{2+} on the resin which was later easily eluted with 2.0 M H_2SO_4 .

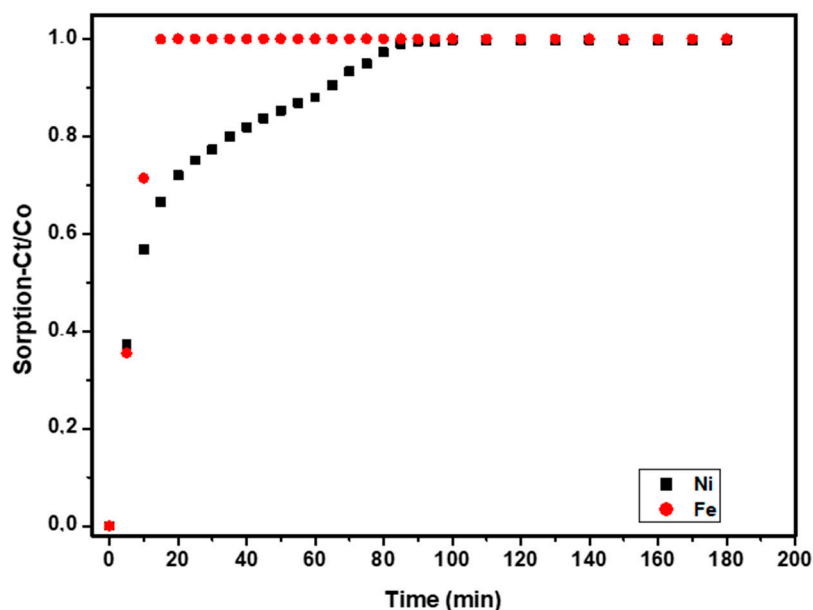


Figure 13. Column sorption of nickel from raffinate solution by spent Dowex M4195 (Conditions: pH 2.0, flowrate—5.0 mL/min and resin bed—20 mm, Cu < 9.0 mg/L, Fe—296 mg/L, Ni—35.1 mg/L, Zn—41.5 mg/L, and Mn—12.05 mg/L, temperature—25 °C).

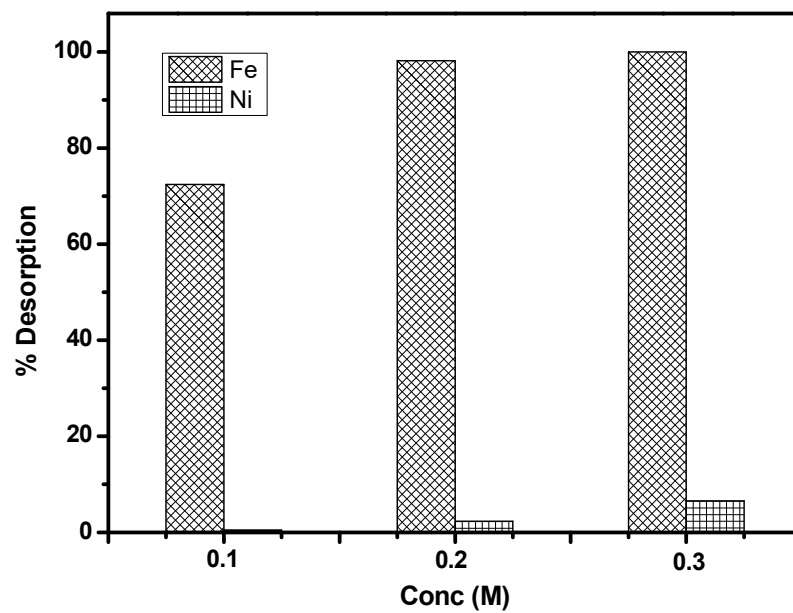


Figure 14. Removal of iron sorbed with Ni²⁺ from spent Dowex M4195 using HCl (Conditions; flow rate 5 mL/min, bed height 20 mm, temperature 25 °C and 30 min).

As the final step of the process, the remaining Fe³⁺ in the raffinate can be easily precipitated using Ca(OH)₂, leaving behind traces of zinc and aluminum in the liquor which can be purified further. The overall process flow for the leaching of PCBs and selective recovery of Cu and Ni and rejecting minor impurities from the leach liquor is shown in Figure 15.

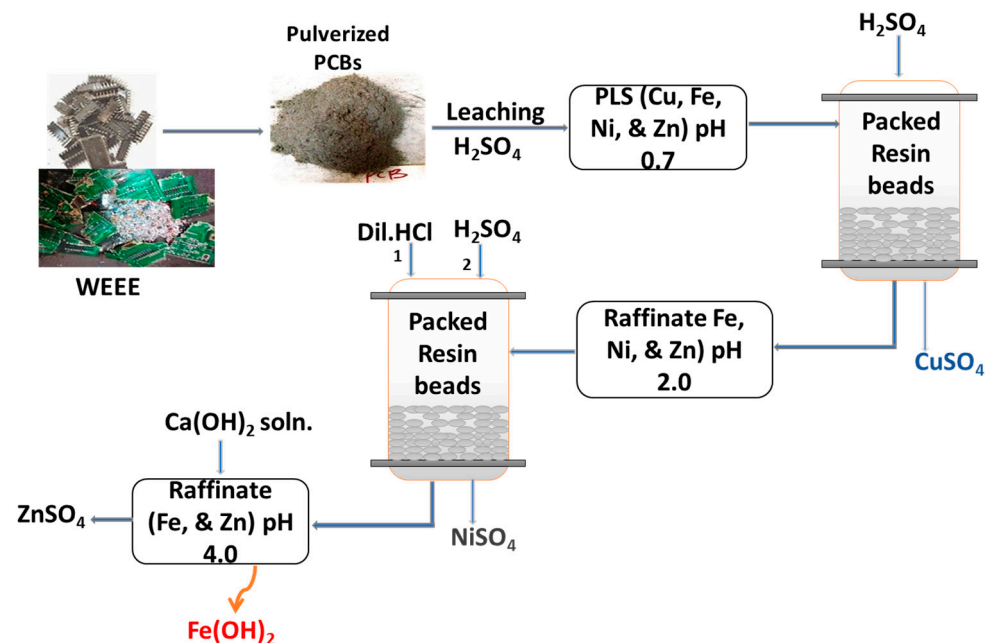


Figure 15. The proposed schematic flow sheet for the sequential recovery of copper, nickel, and zinc from the polymetallic sulfate leach solution of WEEE.

4. Conclusions

In this study, recovery of base metals from mixed metals leach liquor of electronic waste materials via an ion exchange process using Dowex M4195 resin is shown to be feasible in principle. Batch and fixed bed sorption of Cu²⁺ ions on Dowex M4195 resin and removal of Ni²⁺ from raffinate using the spent resin at higher pH were investigated.

The results showed that the resin selectively sorbed Cu^{2+} ions at highly acidic conditions ($\text{pH} < 1.0$). Desorption of Cu^{2+} from resin was achieved with 2.0 M H_2SO_4 . A higher flow rate was found to speed up the breakthrough curve but lead to an overall decrease in Cu^{2+} ion uptake while increasing the bed height delayed the breakthrough curve and more Cu^{2+} uptake was obtained. Adsorption followed both Langmuir and Freundlich isotherm models as well as pseudo-second-order kinetics. The column data modeled indicates that the sorption of Cu^{2+} fitted the Yoon–Nelson model. It was also demonstrated that spent Dowex M4195 could be used further towards Ni^{2+} sorption when contacted with the raffinate from the Cu adsorption step at pH 2, while dilute HCl facilitated selective elution of iron co-sorbed with Ni from the resin, before eluting the Ni again with 2.0 M H_2SO_4 . The Fe^{3+} remaining after Cu and Ni extraction can be precipitated with $\text{Ca}(\text{OH})_2$ leaving a final raffinate free from iron, nickel, and copper for further processing.

Author Contributions: Conceptualization, E.A.A. and V.A.; methodology, E.A.A.; investigation, E.A.A.; writing—original draft preparation, E.A.A.; writing—review and editing, E.A.A., V.A. and J.P.; supervision, V.A. and J.P. All authors have read and agreed to the published version of the manuscript.

Funding: This research was partially funded by the National Research Foundation (NRF) of South Africa through the South African Research Chair in Minerals Beneficiation (Grant UID 64829) as well as the Community of Practice ‘Waste to Value’ (Grant UID 128149). The NRF accepts no liability for the findings presented in this paper.

Data Availability Statement: Data will be made available by the corresponding author on request.

Acknowledgments: Author E.A.A. acknowledges TWAS fellowship for providing financial support. The authors are thankful to the Director, CSIR-Institute of Minerals and Materials technology (IMMT), Bhubaneswar, for providing necessary research facilities during the fellowship and permission to publish the work.

Conflicts of Interest: The authors declare no conflict of interest. The funders had no role in the design of the study; in the collection, analyses, or interpretation of data; in the writing of the manuscript; or in the decision to publish the results.

References

1. Baldé, C.P.; Forti, V.; Gray, V.; Kuehr, R.; Stegmann, P. *The Global E-Waste Monitor 2017: Quantities, Flows, and Resources*; United Nations University: Bonn, Germany; Geneva, Switzerland; Vienna, Austria, 2017.
2. Forti, V.; Baldé, C.P.; Kuehr, R.; Bel, G. *The Global E-Waste Monitor 2020: Quantities, Flows and the Circular Economy Potential*; United Nations University (UNU): Bonn, Germany; United Nations Institute for Training and Research (UNITAR)—Co-hosted SCYCLE Programme, International Telecommunication Union (ITU): Geneva, Switzerland; International Solid Waste Association (ISWA): Rotterdam, The Netherlands, 2020.
3. Luda, M.P. Recycling of Printed Circuit Boards. In *Integrated Waste Management Volume II*; Kumar, S., Ed.; InTech Publishers: London, UK, 2011. Available online: <http://www.intechopen.com/books/integrated-waste-management-volume-ii/recycling-of-printed-circuit-boards> (accessed on 28 September 2023).
4. Das, S.C.; Gopala Krishna, P. Effect of Fe(III) during copper electrowinning at higher current density. *Int. J. Miner. Process.* **1996**, *46*, 91–105. [[CrossRef](#)]
5. Shaw, D.R.; Dreisinger, D.B.; Lancaster, T.; Richmond, G.D.; Tomlinson, M. The commercialization of the FENIX iron control system for purifying copper electrowinning electrolytes. *J. Mater.* **2004**, *56*, 38–41. [[CrossRef](#)]
6. Ehsani, A.; Yazici, E.Y.; Deveci, H. The influence of impurity ions on the electrowinning of copper from waste PCBs leaching solutions. In Proceedings of the XIII International Mineral Processing Symposium (IMPS), Bodrum, Turkey, 10–12 October 2012.
7. Patterson, J.W.; Minear, R.A. Physical-Chemical Methods of Heavy Metal Removal. In *Heavy Metals in the Aquatic Environment*; Kenkel, P.A., Ed.; Pergamon Press: Oxford, UK, 1975; pp. 261–276.
8. Dutrizac, J.E.; Jambor, J.L. Jarosites and Their Application in Hydrometallurgy. *Rev. Mineral. Geochem.* **2000**, *40*, 405–452. [[CrossRef](#)]
9. Arslan, C.; Arslan, F. Thermochemical Review of Jarosite and Goethite Stability Regions at 25 and 95 C. *Eng. Environ. Sci. Acad. J.* **2003**, *27*, 45–52.
10. Yazici, E.Y.; Bas, A.D.; Deveci, H. Removal of Iron as Goethite from Leach Solutions of Waste of Printed Circuit Boards (WPCB). In Proceedings of the 27th International Mineral Processing Congress, Santiago, Chile, 20–24 October 2014.
11. Diniz, C.; Doyle, F.; Ciminelli, V. Effect of pH on the adsorption of selected heavy metal ions from concentrated chloride solutions by chelating resin Dowex M4195. *Sep. Technol.* **2002**, *37*, 3169–3185. [[CrossRef](#)]

12. Habashi, S. *Kinetics of Metallurgical Processes*, 2nd ed.; Metallurgie Extractive Quebec: Quebec, QC, Canada, 1999.
13. Davenport, W.G.I.; King, M.; Schlesinger, M.; Biswas, A.K. *Extractive Metallurgy of Copper*, 5th ed.; Pergamon Press: Oxford, UK, 2011.
14. Dorella, G.; Mansur, M.B. A study of the separation of cobalt from spent Li-ion battery residues. *J. Power Sources* **2007**, *170*, 210–215. [[CrossRef](#)]
15. Long Le, H.; Jeong, J.; Lee, J.C.; Pandey, B.D.; Yoo, J.M.; Huyenh, T.H. Hydrometallurgical process for copper recovery from waste printed circuit boards (PCBs). *Miner. Process. Extr. Metall. Rev.* **2011**, *32*, 90–104. [[CrossRef](#)]
16. Provazi, K.; Campos, B.A.; Espinosa, D.C.R.; Tenório, J.A.S. Metal separation from mixed types of batteries using selective precipitation and liquid-liquid extraction techniques. *Waste Manag.* **2011**, *31*, 59–64. [[CrossRef](#)]
17. Nayl, A.A.; Hamed, M.M.; Rizk, S.E. Selective extraction and separation of metal values from leach liquor of mixed spent Li-ion batteries. *J. Taiwan Inst. Chem. Eng.* **2015**, *55*, 119–125. [[CrossRef](#)]
18. Kumari, A.; Jha, M.K.; Singh, R.P. Recovery of metals from pyrolyzed PCBs by hydrometallurgy techniques. *Hydrometallurgy* **2016**, *165*, 97–105. [[CrossRef](#)]
19. Erust, C.; Akcil, A.; Tuncuk, A.; Deveci, H.; Yazici, Y.E.; Panda, S. A novel approach based on solvent displacement crystallisation for iron removal and copper recovery from solutions of semi-pilot scale bioleaching of WPCBs. *J. Clean. Prod.* **2021**, *294*, 126346. [[CrossRef](#)]
20. Mendes, F.D.; Martins, A.H. Recovery of nickel and cobalt from acid leach pulp by ion exchange using chelating resin. *Miner. Eng.* **2005**, *18*, 945–954. [[CrossRef](#)]
21. Sahni, S.K.; Reedijk, J. Coordination chemistry of chelating resins and ion exchangers. *Coord. Chem. Rev.* **1984**, *59*, 1–139. [[CrossRef](#)]
22. Busche, B.; Wiacek, R.; Davidson, J.; Koonsiripaiboon, V.; Yantasee, W.; Addleman, R.S.; Fryxell, G.E. Synthesis of nanoporous iminodiacetic acid sorbents for binding transition metals. *Inorg. Chem. Commun.* **2009**, *12*, 312–315. [[CrossRef](#)] [[PubMed](#)]
23. Zainol, Z.; Nicol, M. Comparative study of chelating ion exchange resins for the recovery of nickel and cobalt from laterite leach tailings. *Hydrometallurgy* **2009**, *96*, 283–287. [[CrossRef](#)]
24. Laatikainen, K.; Lahtinen, M.; Laatikainen, M.; Paatero, E. Copper removal by chelating adsorption in solution purification of hydrometallurgical zinc production. *Hydrometallurgy* **2010**, *104*, 14–19. [[CrossRef](#)]
25. Hubicki, Z.; Kołodziejka, D. Selective removal of heavy metal ions from waters and waste waters using ion exchange methods. In *Ion Exchange Technologies*; InTech Publishers: London, UK, 2012; p. 193.
26. Kołodziejka, D.; Sofińska-Chmiel, W.; Mendyk, E.; Hubicki, Z. DOWEX M4195 and LEWATIT® MonoPlus TP 220 in heavy metal ions removal from acidic streams. *Sep. Sci. Technol.* **2014**, *49*, 2003–2015. [[CrossRef](#)]
27. Zhu, C.; Liu, F.; Xu, C.; Gao, J.; Chen, D.; Li, A. Enhanced removal of Cu(II) and Ni(II) from saline solution by novel dual-primary-amine chelating resin based on anion-synergism. *J. Hazard. Mater.* **2015**, *287*, 234–242. [[CrossRef](#)]
28. Suwannahong, K.; Sirilamduan, C.; Deepatana, A.; Kreetachat, T.; Wongcharee, S. Characterization and Optimization of Polymeric Bispicolamine Chelating Resin: Performance Evaluation via RSM Using Copper in Acid Liquors as a Model Substrate through Ion Exchange Method. *Molecules* **2022**, *27*, 7210. [[CrossRef](#)]
29. Ajiboye, E.A.; Olasheinde, E.F.; Adebayo, A.O.; Ajayi, O.O.; Ghosh, M.K.; Basu, S. Extraction of copper and zinc from waste printed circuit boards. *Recycling* **2019**, *4*, 36. [[CrossRef](#)]
30. Rusen, A.; Sunkar, A.S.; Topkaya, Y. Zinc and lead extraction from Cinkur leach residues by using hydrometallurgy method. *Hydrometallurgy* **2008**, *93*, 45–50. [[CrossRef](#)]
31. Diniz, C.V.; Ciminelli, V.S.T.; Doyle, F.M. The use of the chelating resin Dowex M-4195 in the adsorption of selected heavy metals ions from manganese solutions. *Hydrometallurgy* **2005**, *78*, 147–155. [[CrossRef](#)]
32. Ajiboye, E.A.; Olasehinde, E.F.; Adebayo, A.O.; Ajayi, O.O. Recovery of Copper and Nickel from Polymetallic Sulphate Leach Solution of Printed Circuit Boards using Dowex M4195. *Physicochem. Probl. Miner. Process.* **2019**, *5*, 1156–1164.
33. Ajiboye, E.A.; Olasehinde, E.F.; Adebayo, A.O.; Ajayi, O.O.; Ghosh, M.K.; Basu, S. Extraction of Cu, Zn, and Ni from waste silica-rich integrated circuits by sulfation roasting and water leaching. *Chem. Pap.* **2020**, *74*, 663–671. [[CrossRef](#)]
34. Wołowicz, A.; Hubicki, Z. Selective adsorption of palladium (II) complexes onto the chelating ion exchange resin Dowex M4195-Kinetic studies. *Solvent Extr. Ion Exch.* **2010**, *28*, 124–159. [[CrossRef](#)]
35. Lara, J.; Tejada, C.; Villabona, Á.; Arrieta, A.; Granados Conde, C. Adsorción de plomo y cadmio en sistema continuo de lecho fijo sobre residuos de cacao. *Rev. Ion* **2017**, *29*, 113–124. [[CrossRef](#)]
36. Grinstead, R. Selective absorption of copper, nickel, cobalt and other transition metal ions from sulphuric acid solutions with the chelating ion exchange resin Dow XFS 4195. *Hydrometallurgy* **1984**, *12*, 387–400. [[CrossRef](#)]
37. Günay, A.; Arslankaya, E.; Tosun, I. Lead removal from aqueous solution by natural and pretreated clinoptilolite: Adsorption equilibrium and kinetics. *J. Hazard. Mater.* **2007**, *146*, 362–371. [[CrossRef](#)]
38. Dąbrowski, A. Adsorption—From theory to practice. *Adv. Colloid Interface Sci.* **2001**, *93*, 135–224. [[CrossRef](#)]
39. Ayawei, N.; Ebelegi, A.N.; Wankasi, D. Modelling and interpretation of adsorption isotherms. *J. Chem.* **2017**, *2017*, 3039817. [[CrossRef](#)]
40. Boparai, H.K.; Joseph, M.; O’Carroll, D.M. Kinetics and thermodynamics of cadmium ion removal by adsorption onto nano zerovalent iron particles. *J. Hazard. Mater.* **2011**, *186*, 458–465. [[CrossRef](#)] [[PubMed](#)]

41. Samadi, N.; Ansari, R.; Khodavirdilo, B. Removal of Copper ions from aqueous solutions using polymer derivations of poly (styrene-alt-maleic anhydride). *Egypt. J. Pet.* **2016**, *26*, S1110062116300320. [[CrossRef](#)]
42. Fotalan, C.M.; Kan, C.-C.; Dalida, M.L.; Pascua, C.; Wan, M.-W. Fixed-bed column studies on the removal of copper using chitosan immobilized on bentonite. *Carbohydr. Polym.* **2011**, *83*, 697–704. [[CrossRef](#)]
43. Revathi, M.; Saravanan, M.; Chiya, A.B.; Velan, M. Removal of Copper, Nickel, and Zinc Ions from Electroplating Rinse Water. *Clean Soil Air Water* **2012**, *40*, 66–79. [[CrossRef](#)]
44. Rudnicki, P.; Hubicki, Z.; Kołodyńska, D. Evaluation of heavy metal ions removal from acidic wastewater streams. *Chem. Eng. J.* **2014**, *252*, 362–373. [[CrossRef](#)]
45. Perez, I.D.; Correa, M.M.J.; Cianga Silvas, F.P.; Tenório, J.A.S.; Espinosa, D.C.R. Effect of Flow Rate on Metals Adsorption of Synthetic Solution Using Chelating Resin Dowex XUS43605 in Column Experiments. In *Energy Technology*; Springer: Berlin/Heidelberg, Germany, 2017; pp. 483–491. [[CrossRef](#)]
46. Lim, A.P.; Aris, A.Z. Continuous fixed-bed column study and adsorption modeling: Removal of cadmium (II) and lead (II) ions in aqueous solution by dead calcareous skeletons. *Biochem. Eng. J.* **2014**, *87*, 50–61. [[CrossRef](#)]
47. Punrattanasin, P.; Sariem, P. Adsorption of Copper, Zinc, and Nickel using Loess as Adsorbent by Column Studies. *Pol. J. Environ. Stud.* **2015**, *24*, 1259–1266. [[CrossRef](#)] [[PubMed](#)]
48. Jacobs, J.C.; Groot, D.R. Improving cathode morphology at a copper electrowinning plant by optimizing Magnafloc 333 and chloride concentrations. *J. S. Afr. Inst. Min. Metall.* **2019**, *119*, 983–987. [[CrossRef](#)]
49. Beukes, N.; Badenhorst, J. Copper electrowinning: Theoretical and practical design. *J. S. Afr. Inst. Min. Metall.* **2009**, *106*, 343–356.
50. Wołowicz, A.; Hubicki, Z. Enhanced removal of copper (II) from acidic streams using functional resins: Batch and column studies. *J. Mater. Sci.* **2020**, *55*, 13687–13715. [[CrossRef](#)]
51. Verduzco-Navarro, I.P.; Rios-Donato, N.; Jasso-Gastinel, C.F.; Martinez-Gomez, A.D.J.; Mendizábal, E. Removal of Cu (II) by fixed-bed columns using Alg-Ch and Alg-ChS hydrogel beads: Effect of operating conditions on the mass transfer zone. *Polymers* **2020**, *12*, 2345. [[CrossRef](#)]
52. Zimmerman, M.D.; Bennett, P.C.; Sharp, J.M., Jr.; Choi, W.J. Experimental determination of sorption in fractured flow systems. *J. Contam. Hydrol.* **2002**, *58*, 51–77. [[CrossRef](#)] [[PubMed](#)]
53. Yahorava, V.; Kotze, M.; Auerswald, D. Evaluation of different adsorbents for copper removal from cobalt electrolyte. *J. S. Afr. Inst. Min. Metall.* **2014**, *114*, 383–390.
54. Angel, V.; Candelaria, T.; Rodrigo, O.; Keily, P.; Ciro, B. Impact of temperature, bed height, and particle size on Ni (II) removal in a continuous system: Modelling the break curve. *Pol. Acad. Sci.* **2022**, *52*, 257–264.

Disclaimer/Publisher’s Note: The statements, opinions and data contained in all publications are solely those of the individual author(s) and contributor(s) and not of MDPI and/or the editor(s). MDPI and/or the editor(s) disclaim responsibility for any injury to people or property resulting from any ideas, methods, instructions or products referred to in the content.